

Dynamics of photo-doped charge transfer insulators

Denis Golež,¹ Lewin Boehnke,^{1,*} Martin Eckstein,² and Philipp Werner¹

¹*Department of Physics, University of Fribourg, 1700 Fribourg, Switzerland*

²*Department of Physics, University of Erlangen-Nürnberg, 91058 Erlangen, Germany*

We study the dynamics of charge-transfer insulators after photo-excitation using the three-band Emery model and a nonequilibrium extension of Hartree-Fock+EDMFT and GW+EDMFT. While the equilibrium properties are accurately reproduced by the Hartree-Fock treatment of the full p bands, dynamical correlations are essential for a proper description of the photo-doped state. The insertion of doublons and holons leads to a renormalization of the charge transfer gap and to a substantial broadening of the bands. We calculate the time-resolved photoemission spectrum and optical conductivity and find qualitative agreement with experiments. Our formalism enables the realistic description of nonequilibrium phenomena in a large class of charge-transfer insulators, and provides a tool to explore the optical manipulation of interaction and correlation effects.

PACS numbers: 05.70.Ln

The ability to engineer the microscopic parameters of correlated electron materials is important for the understanding of their complex properties and for technological applications. An example is the control of superconductivity by pressure, doping or strain [1–3] under equilibrium conditions. Recent progress in ultrafast laser techniques motivates new strategies which involve nonthermal states. Experiments have demonstrated, e.g., the switching to a hidden metallic state in 1T-TaS₂ [4], or light-induced enhancement of superconductivity [5, 6] and excitonic order [7]. Related are theoretical proposals to modify the band structure [8, 9] or interactions by electronic excitations [10–12] or phonon driving [13–18].

A simple way to change the properties of correlated materials is the photo-excitation of charge carriers across a Mott or charge transfer (CT) gap. When it comes to nonequilibrium simulations most of the theoretical work related to Mott insulators has focused on single-band models [19–26], which miss important aspects of the physics of CT insulators with p and d bands. In these compounds, photo-excitation results in doublon and holon charge carriers of a qualitatively different nature, and depending on the excitation energy one may selectively excite electrons from occupied p or d states. Furthermore, photo-doping may change the relative position of the p and d bands with a potentially large impact on the low-energy properties.

A paradigmatic class of materials where this plays a role are the cuprates. The equilibrium properties of cuprates have been investigated with a broad range of methods including exact diagonalization [27, 28], dynamical mean field theory (DMFT) [29–31] and its cluster extensions [32]. These studies emphasized the importance of a multiband description including p orbitals [33, 34] and the role of spin [32] and charge fluctuations [35, 36]. Photoexcitation with typical 1.5 eV or 3 eV laser pulses can clearly reveal the multi-band physics, even though the equilibrium properties are partially captured by a single-band model. In fact, pump-probe studies on cuprate superconductors have detected photo-induced band shifts and modifications in effective masses [37–42], as well as a redistribution of spectral weight between different characteristic energy scales [43, 44].

In this work, we consider the two-dimensional three-band Emery model [45] describing the Cu $d_{x^2-y^2}$ (denoted d) and O p_x and p_y orbitals, where the O orbitals lie between Cu ions forming a square lattice with lattice constant a . The three terms of the Hamiltonian $H = H_e + H_{\text{kin}} + H_{\text{int}}$ are

$$\begin{aligned} H_e &= \epsilon_d \sum_i n_i^d + (\epsilon_d + \Delta_{pd}) \sum_{i,\delta} n_i^p, \\ H_{\text{kin}} &= \sum_{ij\sigma} \sum_{(\alpha,\beta) \in (d,p_x,p_y)} t_{ij}^{\alpha\beta} c_{i\alpha\sigma}^\dagger c_{j\beta\sigma}, \\ H_{\text{int}} &= \sum_{ij} \sum_{(\alpha,\beta) \in (d,p_x,p_y)} V_{ij}^{\alpha\beta} n_i^\alpha n_j^\beta, \end{aligned}$$

with $V_{ij}^{\alpha\beta} = U_{dd}$ if $i = j$ and $\alpha = \beta = d$, and $V_{ij}^{\alpha\beta} = \frac{1}{2}U_{dp}$ for nearest-neighbor d and p orbitals. The crystal field splitting Δ_{dp} determines the difference between the on-site energy for the d orbital, ϵ_d , and that for the p orbitals, $\epsilon_d + \Delta_{dp}$. We denote the nearest neighbor hopping between the d and p_x, p_y orbitals by t^{dp} and between the p_x and p_y orbitals by t^{pp} , while $-t_{ii}^{\alpha\alpha} = \mu$ is the chemical potential.

We solve this lattice problem using the fully self-consistent GW+EDMFT [11, 46–48] and Hartree-Fock (HF)+EDMFT methods, which are based on extended dynamical mean field theory (EDMFT) [10, 47–49], and a non-crossing approximation impurity solver [10]. Since the local interactions in the d orbital are stronger than in the p orbitals, we restrict the correlated subspace (EDMFT treatment) to the d -orbital, while the p orbitals are treated at the HF or GW level. This approach requires a downfolding from the three-orbital space of the full model to the d orbital correlated subspace, which has to be implemented at the level of the electronic Green's function and the (bosonic) screened interaction.

The dynamics of the system is described in terms of the momentum and orbital resolved electronic Green's function $G_{k\sigma}^{\alpha\beta}(t, t') = -i\langle T_C c_{k\alpha\sigma}(t) c_{k\beta\sigma}^\dagger(t') \rangle$ and the charge correlation function $\chi_q^{\alpha\beta}(t, t') = -i\langle T_C \tilde{n}_{q\alpha}(t) \tilde{n}_{-q\beta}(t') \rangle$, which determines the inverse of the orbital-resolved dielectric function $[\epsilon_q^{-1}] = I + v_q * \chi_q$ and the screened interaction $W_q = [\epsilon_q^{-1}] * v_q$, where v_q is the Fourier transform of the

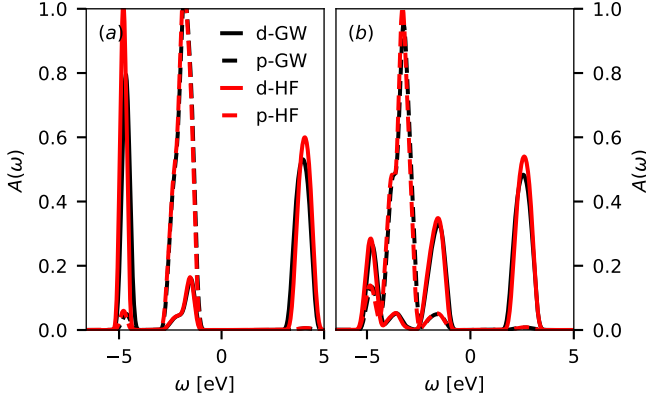


Figure 1. Orbitaly resolved spectral function obtained in the GW+EDMFT (black) and HF+EDMFT (red) approximation for the CT (a) and LCO (b) set-ups. The full (dashed) lines represent the d (p_x and p_y) orbitals.

bare interaction. The mapping of the lattice problem to an impurity problem and the downfolding procedure lead to a retarded density-density interaction $\mathcal{U}(t, t')$ on the impurity (d orbital), which is related to the screened interaction by $W_{\text{loc}}^{dd} = \mathcal{U} + \mathcal{U} * \chi_{\text{imp}} * \mathcal{U}$.

The electromagnetic field leads to an acceleration of the charge carriers as well as dipolar transitions. The gauge invariant description of both effects is given by the modified hopping term [50, 51]

$$H_{\text{kin}} = \sum_{\substack{ij\sigma, (\alpha, \beta) \\ \in (d, p_x, p_y)}} (t_{ij}^{\alpha\beta} + \vec{E} \cdot \vec{D}_{ij}^{\alpha\beta}) e^{-i\varphi_{ij}} c_{i\alpha\sigma}^\dagger c_{j\beta\sigma}, \quad (1)$$

where $\varphi_{ij} = e/\hbar \int_{R_i}^{R_j} d\vec{r} \vec{A}(\vec{r}, t)$ is the Peierls phase and $\vec{A}(\vec{r}, t)$ is the vector potential, which is related to the electric field by $\vec{E}(\vec{r}, t) = -\partial_t \vec{A}(\vec{r}, t)$. We assume that $\vec{A}(t)$ and $\vec{E}(t)$ are homogeneous in space. For a quantitative description of the photo-excitation in multiband materials the dipolar matrix elements will have to be obtained from ab-initio calculations. In the following simulations, we use nearest neighbor d to p dipolar matrix elements $D \equiv D_{(i, \{0,0\})(i, \{a/2, 0\})}^{p_x d} = -D_{(i, \{0,0\})(i, \{a/2, 0\})}^{p_y d} = 0.3 \text{ e}\text{\AA}$. We have checked that the results do not qualitatively dependent on the value of D .

We will study two characteristic set-ups previously considered in the literature: i) a charge transfer insulator close to the atomic limit, where a strong Coulomb repulsion opens a large Mott gap and narrow p bands lie well separated between the lower and the upper Hubbard bands (“CT case”), and ii) the parameter regime relevant for La_2CuO_4 , as obtained from LDA calculations and the constrained RPA downfolding procedure to the low energy space composed of the d and p orbitals [35] (“LCO case”). In this set-up the p bands lie in the same energy range as the lower Hubbard band. We parametrise the tight-binding Hamiltonian following Ref. 33.

In Fig. 1 we present the orbitaly resolved local spectral functions $A_\alpha(\omega) = -\frac{1}{\pi} \text{Im}[G_{\text{loc}}^{\alpha, \alpha}(\omega)]$, for $\alpha = d, p_x, p_y$. In all

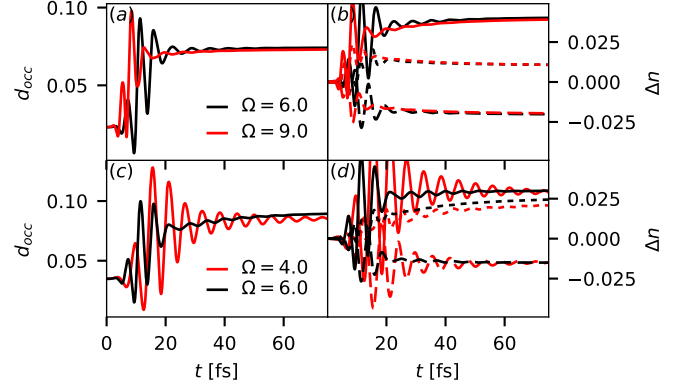


Figure 2. Dynamics after photo-excitation for the CT (top panels) and LCO (bottom panels) set-up. The left panels show the change of the double occupancy d_{occ} , while the right panels plot the change in the occupation of the d (full line) and p_x (p_y) (dashed line) orbitals. Dotted lines show the density of holes in the lower Hubbard band.

calculations we set the inverse temperature to $\beta = 5.0$, which is above the Néel temperature. In the CT case (Fig. 1(a)), with parameters $U_{dd} = 8.0 \text{ eV}$, $U_{dp} = 2.0 \text{ eV}$, $t_{dp} = 0.4 \text{ eV}$, $t_{dd} = -0.1 \text{ eV}$, $t_{pp} = 0.15 \text{ eV}$, $\Delta_{pd} = -2.0 \text{ eV}$, the lower Hubbard band is well separated from the p bands. Due to the hopping between the d and p orbitals there is a hybridisation which pushes the lower Hubbard band further down in energy. In the example relevant for La_2CuO_4 (Fig. 1(b)), with parameters $U_{dd} = 5.0 \text{ eV}$, $U_{dp} = 2.0 \text{ eV}$, $t_{dp} = 0.5 \text{ eV}$, $t_{dd} = -0.1 \text{ eV}$, $t_{pp} = 0.15 \text{ eV}$, $\Delta_{pd} = -3.5 \text{ eV}$, the spectral function below the Fermi level is split into three distinct peaks: a peak at $\omega = -3.3 \text{ eV}$ of predominantly p orbital character, the bonding band corresponding to the Zhang-Rice singlet around $\omega = -1.6 \text{ eV}$, and the anti-bonding band pushed to lower energy, with a center at $\omega = -4.9 \text{ eV}$. In equilibrium, the GW+EDMFT and HF+EDMFT spectra are almost indistinguishable, which shows that static correlations are sufficient for the treatment of the fully occupied p orbitals. We also note that the gap suppresses the effect of screening [52], so that the GW self-energy and polarization results in only a tiny reduction of the effective static interaction (and hence of the gap): $\mathcal{U}(\omega = 0) - U_{dd} \approx -0.03 \text{ eV}$ for the CT and -0.05 eV for the LCO set-up.

We now turn to the photo-excitation and the subsequent relaxation. A short pulse $E(t) = E_0 e^{-4.6(t-t_0)^2/t_0^2} \sin(\Omega(t-t_0))$ polarized along the (11) direction creates doubly occupied d orbitals as evidenced by an enhanced population of the upper Hubbard band, see Fig. 2. The width of the pulse $t_0 = 2\pi n/\Omega$ is chosen such that the envelope accommodates $n = 2$ cycles. Due to the mixed nature of the states below the Fermi level one may expect that the ratio between the excited electrons originating from the p or d orbital depends on the frequency of the pulse. In the following we will choose frequencies corresponding to a photo-excitation from the characteristic features in the occupied part of the spectrum to the upper Hubbard band and adjust the excitation strength

of the pulse E_0 at each given frequency such that the number of photo-doped doublons and holons is approximately 5%.

In Fig. 2(a) we present the time evolution of the double occupancy in the CT set-up for two different frequencies corresponding to the transitions from the p band ($\Omega = 6, E_0 = 0.37$) and the lower Hubbard band ($\Omega = 9, E_0 = 0.87$) to the upper Hubbard band. Due to the large gap size the number of doubly occupied sites changes only very slowly after the photo-excitation [23, 26, 53, 54]. The change in the occupation of the orbitals (Fig. 2(b)) shows that charge is transferred from the p to the d orbital for both excitations. The dotted lines in Fig. 2(b) indicate the density of holes in the lower Hubbard band, $\Delta d_{\text{occ}} - 2\Delta n_p$. The final occupations are remarkably independent of the excitation frequency. The spectrally resolved occupation (not shown) indicates that after an ultra-fast redistribution of occupation between the region of the lower Hubbard band and the p -band the holes predominantly reside in the p -band. This inter-band decay is only described within the GW+DMFT formalism and not by HF+DMFT, so that its likely origin is the strong coupling of electrons to charge fluctuations. The response is similar to the single band extended Hubbard model deep in the Mott phase, where the doublons quickly relax to the lower edge of the upper Hubbard band via the emission of plasmonic excitations [10]. This observation shows that the correct description of the photo-excited state already a few fs after the excitation, and of orbital selectivity, requires an accurate treatment of the dynamic charge fluctuations.

In the LCO case we excite electrons to the upper Hubbard band either from the ZR singlet ($\Omega = 4, E_0 = 0.54$) or from the band with dominant p character ($\Omega = 6.0, E_0 = 0.31$). Due to the smaller gap size, impact-ionization processes become important and lead to a more rapid increase of the double occupancy after the photo-excitation [55]. For a fixed number of doubly occupied sites (Fig. 2(d)) there is a larger percentage of holes in the d orbitals than for the CT insulator (dashed lines). The holes predominantly occupy the ZR band as seen in the greater component of the orbitally resolved spectral function (not shown). Apart from strong initial oscillation due to the p - d hybridization the final occupation is again remarkably independent of Ω .

We next discuss the time evolution of the spectrum after the photo-excitation by analyzing the partial Fourier transform of the orbitally resolved spectral function $A_\alpha(\omega, t) = -(1/\pi)\text{Im}[\int_t^{t+t_{\text{cut}}} dt' e^{i\omega(t'-t)} G_\alpha^R(t', t)]$, with $t_{\text{cut}} = 8$ and $\alpha \in \{d, p_x, p_y\}$. Again we will compare the GW+EDMFT and HF+EDMFT approximations in order to address the role of nonlocal charge fluctuations. Due to the Coulomb interaction U_{dp} between the holes in the p orbitals and the doublons in the d orbital there is an almost instantaneous reduction of the gap between the p band and the upper Hubbard band, see Fig. 3. It originates from the static Hartree-Fock attraction and is determined by the change in the local orbital occupancy [42] $\Delta \Sigma_{dd}^H = (U_{dd} - 2U_{dp})\Delta n_d$, where the factor of 2 originates from the number of nearest-neighbor p orbitals and we have used the conservation of the total charge

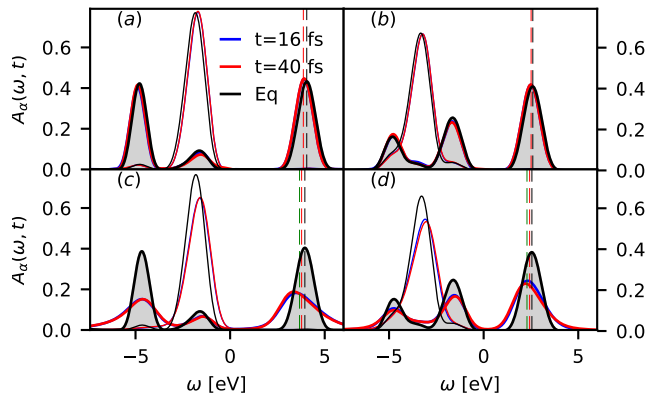


Figure 3. Time evolution of the spectral function $A_\alpha(\omega, t)$ within HF+EDMFT ((a) and (b)) and GW+EDMFT ((c) and (d)) for the CT (left panels) and LCO (right panels) set-ups, both excited with the pulse frequency $\Omega = 6.0$. The black lines show the equilibrium spectra. Thick shaded (thin) lines represent the d (p_x and p_y) orbitals. The black vertical line marks the peak position in equilibrium, the red line indicates the shift of the band due to the reduced static Hartree interaction and the green line corresponds to the combined effect of Hartree shift and static reduction of the effective impurity interaction $\mathcal{U}(\omega = 0)$.

$\Delta n_d = -(\Delta n_{p_x} + \Delta n_{p_y})$. The contribution of this effect to the shrinking gap is indicated in Fig. 3 by the vertical red line, $\Delta \Sigma_{dd}^H = -0.15$ (-0.17) eV for the CT (LCO) case.

Going beyond the HF description, the inclusion of nonlocal charge fluctuations leads to: a) a further reduction of the gap size and a *band shift*, and b) a *substantial broadening* of the spectra (in particular for the d orbitals) due to a strong electron-plasmon coupling (compare the GW+EDMFT and HF+EDMFT results in Fig. 3). Both effects are a consequence of the photo-induced changes in the screening. The additional gap shrinking can be quantified by the reduced static interaction, $\mathcal{U}(\omega = 0) - U_{dd} \approx -0.14$ eV for both set-ups, which is indicated by the green vertical line in Fig. 3. One can see that the full reduction of the gap cannot be described by these static contributions alone and must be attributed to dynamical screening and doping effects. By analyzing the momentum-dependent spectrum we confirmed that the broadening of the local (momentum-averaged) spectrum originates mainly from a strong increase in the linewidth due to the electron-plasmon coupling and to a much lesser extent from a modification of the effective velocities. Comparing Fig. 3 with Fig. 1 we conclude that the treatment of both dynamic screening and the feedback of the nonlocal charge fluctuations is qualitatively important for the description of the photo-excited state, while these effects are negligible in equilibrium [56].

The dynamics of the p band exhibits a remarkable resemblance with recent time-resolved ARPES data, which show a non-thermal broadening of the $2p_\pi$ band in the antinodal direction of optimally doped Y-Bi2212 [42]. The interpretation of Ref. 42, which attributed the non-thermal changes in the experimental spectra to nonlocal charge fluctuations, is fully consistent with our results.

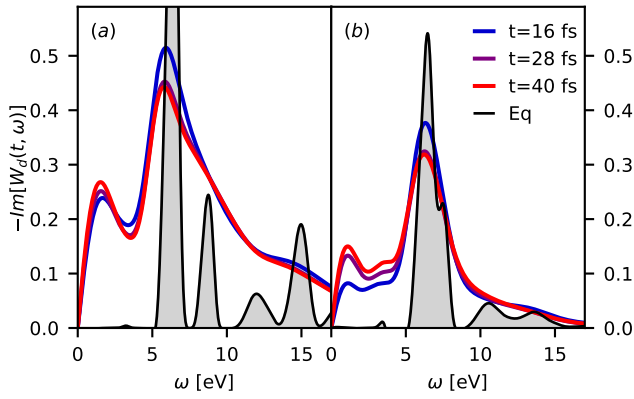


Figure 4. Time evolution of the screened interaction $W_d(t, \omega)$ for the CT (a) and LCO (b) set-up, both excited with frequency $\Omega = 6.0$. The black shaded lines represent the equilibrium spectrum.

The information about the time-dependent changes in the screening properties of the d orbital is contained in the screened interaction $W_d(\omega, t)$, see Fig. 4. The equilibrium screening modes for the charge-transfer insulator include i) a peak at $\omega_{CT} \approx 6$ corresponding to particle-hole excitations from the p band to the upper Hubbard band, and ii) a peak at $\omega_H \approx 8.5$ matching the excitations from the lower to the upper Hubbard band, and higher order excitations [see also Fig. 1(a)]. After the photo-excitation these features are smeared out and a continuum of screening modes appears at low energies. These are associated with charge excitations within the photo-doped bands and result in an additional screening [10]. Within EDMFT one can define an effective coupling of the electrons and the charge fluctuations from the integral over $\text{Im}\mathcal{U}(\omega)/\omega$ (or, equivalently, the reduction of $\text{Re}\mathcal{U}(\omega = 0)$) [10, 11, 47]. The coupling strength to the photo-induced charge fluctuations at $\omega \lesssim 6$, $\lambda_{\text{ind}} = 2 \int_0^6 d\omega (-\text{Im}[\mathcal{U}(\omega)]/\omega) \approx 0.16$, corresponds to a rather strong coupling, which explains the substantial broadening of the spectra in Fig. 3. The dynamics of $W_d(t, \omega)$ in the LCO case is qualitatively similar except for an additional peak at $\omega \approx 3.5$, which originates from the charge excitations between the Zhang-Rice singlet and the lower edge of the upper Hubbard band. The effective electron-plasmon coupling $\lambda_{\text{ind}} \approx 0.17$ is comparable to the CT case.

Finally, we discuss the signature of the band-gap renormalization in the optical conductivity. We explicitly simulate a probe pulse along the (11) direction and extract the photo-induced current as the difference in the current with and without a probe pulse, $j_{\text{probe}} = j_{\text{pump+probe}} - j_{\text{pump}}$. For a weak probe pulse the optical conductivity can be evaluated as the ratio $\sigma(\omega, t_p) = j(\omega, t_p)/E(\omega, t_p)$, where $X(\omega, t_p) = \int_0^{t_{\text{cut}}} ds X(t+s)e^{-i\omega s}$ is the Fourier transform of $X = j, E$, and t_p is the center of the probe pulse. This procedure avoids the calculation of the current-current correlation function including vertex corrections. We apply both the pump and probe pulses in the (11) direction.

The optical conductivity in equilibrium (black lines) and

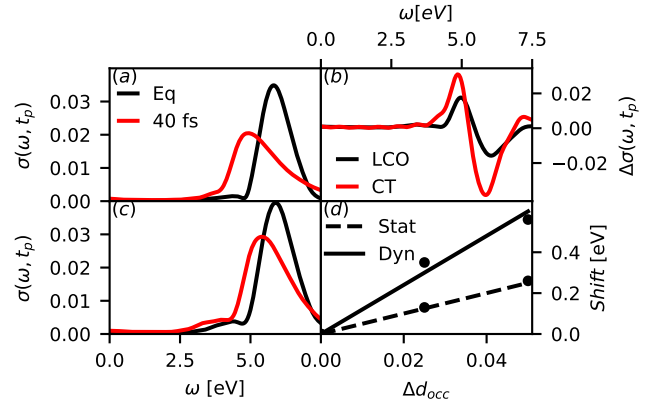


Figure 5. Time-dependent optical conductivity in the (11) direction $\sigma(\omega, t_p)$ for the CT (a) and LCO (c) set-up. The black lines represent the equilibrium data, where we used an additional damping factor $\eta = 0.25$ to smoothen artifacts of the Fourier transform due to the finite time window. (b) The difference from the equilibrium result $\Delta\sigma(t_p, \omega) = \sigma(t_p, \omega) - \sigma^{\text{eq}}(\omega)$ for the delayed probe pulse $t_p = 40$ fs in both set-up. (d) The gap size renormalization at the position of the half-maximum in the optical conductivity (Dyn) as a function of the photo-excited doublons and comparison with the renormalization expected from the static shift (Stat) $\Sigma_H + \mathcal{U}(\omega = 0)$.

for $t_p = 40$ fs after the pump pulse is presented in Fig. 5(a,c). The equilibrium optical conductivity for both cases exhibits a main peak corresponding to excitations from the p band to the upper Hubbard band. In the LCO case, see Fig. 5(c), the small peak at $\omega = 4.4$ eV corresponds to excitations from the ZR singlet to the upper Hubbard band.

After the photo-excitation the optical conductivity shows a clear shift toward lower energies, originating from the HF shift and the enhanced screening. In order to highlight this evolution we also plot the change of the optical conductivity from the equilibrium value (Fig. 5(b)) as it is usually done in the experimental literature [41]. Indeed, a characteristic shift of the excitation gap to lower energies has been reported in a number of pump-probe experiments on cuprates and other charge transfer insulators, see for instance Refs. 38–41, and 57. The comparison of the shift to the static screening contribution (line labeled “Stat” in Fig. 5(d)) shows that more than 50% of the gap renormalization is due to the broadening of the bands. A recent experimental study of photo-doped La_2CuO_4 [41] reports an even somewhat larger shift than predicted by the line labeled “Dyn” in Fig. 5(d). This suggests that dynamical effects, including the substantial broadening of the bands in the photo-doped state, are essential for a quantitative description of photo-doped cuprates.

In conclusion, we have studied the pump-probe dynamics of the 3-band Emery model, relevant for a large family of charge-transfer insulators, using nonequilibrium GW+EDMFT and HF+EDMFT. The electric field pulse transfers charge from the p bands to the upper Hubbard band, which results in relative band shifts. Similar band shifts have been observed in a recent TDDFT+U study of NiO [12], while the present study shows that the dynamical screening strongly

enhances this effect. The strong plasmon coupling in the photo-doped state leads to a substantial broadening of the d and p bands, which implies that dynamical correlation effects (beyond HF) are essential for the description of the ligand bands, in contrast to equilibrium.

The electronic structure of the Zhang-Rice singlet determines the low-energy magnetic properties of the system. The photo-induced shift may have profound consequences on the magnetic correlations in these systems, which makes the investigation of photo-induced changes in the magnetic correlations an interesting topic for future studies. On the methodological side, our work represents a crucial step toward the *ab-initio* description of strongly correlated systems out of equilibrium, where the material-specific input is obtained via a multi-tier approach analogous to the scheme recently demonstrated for equilibrium systems in Refs. [35, 58, 59].

We thank Y. Murakami and A. J. Millis for useful discussions, and M. Schüler for numerous advises on computational issues. The calculations have been performed on the Beo04 and Beo05 clusters at the University of Fribourg. DG and PW acknowledge support from SNSF Grant No. 200021_165539 and ERC Consolidator Grant No. 724103. ME acknowledges financial support from ERC Starting Grant No. 716648.

* Now at Crypto Finance AG

- [1] B. Sipos, A. F. Kusmartseva, A. Akrap, H. Berger, L. Forró, and E. Tutiš, *Nature materials* **7**, 960 (2008).
- [2] R. H. Zadik, Y. Takabayashi, G. Klupp, R. H. Colman, A. Y. Ganin, A. Potočník, P. Jeglič, D. Arčon, P. Matus, K. Kamarás, Y. Kasahara, Y. Iwasa, A. N. Fitch, Y. Ohishi, G. Garbarino, K. Kato, M. J. Rosseinsky, and K. Prasad, *Science Advances* **1** (2015), 10.1126/sciadv.1500059, <http://advances.sciencemag.org/content/1/3/e1500059.full.pdf>.
- [3] O. Ivashko, M. Horio, W. Wan, N. Christensen, D. McNally, E. Paris, Y. Tseng, N. Shaik, H. Rønnow, H. Wei, *et al.*, arXiv preprint arXiv:1805.07173 (2018).
- [4] L. Stojchevska, I. Vaskivskiy, T. Mertelj, P. Kusar, D. Svetin, S. Brazovskii, and D. Mihailovic, *Science* **344**, 177 (2014).
- [5] D. Fausti, R. I. Tobey, N. Dean, S. Kaiser, A. Dienst, M. C. Hoffmann, S. Pyon, T. Takayama, H. Takagi, and A. Cavalleri, *Science* **331**, 189 (2011), <http://www.sciencemag.org/content/331/6014/189.full.pdf>.
- [6] M. Mitrano, A. Cantaluppi, D. Nicoletti, S. Kaiser, A. Perucchi, S. Lupi, P. Di Pietro, D. Pontiroli, M. Riccò, S. R. Clark, *et al.*, *Nature* **530**, 461 (2016).
- [7] S. Mor, M. Herzog, D. Golež, P. Werner, M. Eckstein, N. Katayama, M. Nohara, H. Takagi, T. Mizokawa, C. Monney, and J. Stähler, *Phys. Rev. Lett.* **119**, 086401 (2017).
- [8] T. Oka and H. Aoki, *Phys. Rev. B* **79**, 081406 (2009).
- [9] Y. H. Wang, H. Steinberg, P. Jarillo-Herrero, and N. Gedik, *Science* **342**, 453 (2013), <http://science.sciencemag.org/content/342/6157/453.full.pdf>.
- [10] D. Golež, M. Eckstein, and P. Werner, *Phys. Rev. B* **92**, 195123 (2015).
- [11] D. Golež, L. Boehnke, H. U. R. Strand, M. Eckstein, and P. Werner, *Phys. Rev. Lett.* **118**, 246402 (2017).
- [12] N. Tancogne-Dejean, M. A. Sentef, and A. Rubio, ArXiv e-prints (2017), arXiv:1712.01067 [cond-mat.str-el].
- [13] M. Knap, M. Babadi, G. Refael, I. Martin, and E. Demler, *Phys. Rev. B* **94**, 214504 (2016).
- [14] M. Babadi, M. Knap, I. Martin, G. Refael, and E. Demler, *Phys. Rev. B* **96**, 014512 (2017).
- [15] Y. Murakami, N. Tsuji, M. Eckstein, and P. Werner, *Phys. Rev. B* **96**, 045125 (2017).
- [16] G. Mazza and A. Georges, *Phys. Rev. B* **96**, 064515 (2017).
- [17] D. M. Kennes, E. Y. Wilner, D. R. Reichman, and A. J. Millis, *Nature Physics* **13**, 479 (2017).
- [18] Y. Murakami, D. Golež, M. Eckstein, and P. Werner, *Phys. Rev. Lett.* **119**, 247601 (2017).
- [19] H. Aoki, N. Tsuji, M. Eckstein, M. Kollar, T. Oka, and P. Werner, *Rev. Mod. Phys.* **86**, 779 (2014).
- [20] M. Eckstein and P. Werner, *Scientific reports* **6** (2016).
- [21] M. Eckstein and P. Werner, ArXiv e-prints (2014), arXiv:1410.3956 [cond-mat.str-el].
- [22] M. Eckstein and P. Werner, *Phys. Rev. Lett.* **110**, 126401 (2013).
- [23] M. Eckstein and P. Werner, *Phys. Rev. B* **84**, 035122 (2011).
- [24] D. Golež, J. Bonča, M. Mierzejewski, and L. Vidmar, *Phys. Rev. B* **89**, 165118 (2014).
- [25] S. Dal Conte, L. Vidmar, D. Golež, M. Mierzejewski, G. Soavi, S. Peli, F. Banfi, G. Ferrini, R. Comin, B. M. Ludbrook, *et al.*, *Nat. Phys.* **11**, 421 (2015).
- [26] Z. Lenarčič and P. Prelovšek, *Phys. Rev. Lett.* **111**, 016401 (2013).
- [27] J. Jaklič and P. Prelovšek, *Adv. Phys.* **49**, 1 (2000).
- [28] T. Tohyama, *Phys. Rev. B* **70**, 174517 (2004).
- [29] A. Comanac, L. deMedici, M. Capone, and A. Millis, *Nature Physics* **4**, 287 (2008).
- [30] L. de' Medici, X. Wang, M. Capone, and A. J. Millis, *Phys. Rev. B* **80**, 054501 (2009).
- [31] C. Weber, K. Haule, and G. Kotliar, *Phys. Rev. B* **78**, 134519 (2008).
- [32] Q. Yin, A. Gordienko, X. Wan, and S. Y. Savrasov, *Phys. Rev. Lett.* **100**, 066406 (2008).
- [33] P. Hansmann, N. Parragh, A. Toschi, G. Sangiovanni, and K. Held, *New Journal of Physics* **16**, 033009 (2014).
- [34] H. Ebrahimnejad, G. A. Sawatzky, and M. Berciu, *Nature Physics* **10**, 951 (2014).
- [35] P. Werner, R. Sakuma, F. Nilsson, and F. Aryasetiawan, *Phys. Rev. B* **91**, 125142 (2015).
- [36] P. Werner and M. Casula, *Journal of Physics: Condensed Matter* **28**, 383001 (2016).
- [37] J. D. Rameau, S. Freutel, L. Rettig, I. Avigo, M. Ligges, Y. Yoshida, H. Eisaki, J. Schneeloch, R. D. Zhong, Z. J. Xu, G. D. Gu, P. D. Johnson, and U. Bovensiepen, *Phys. Rev. B* **89**, 115115 (2014).
- [38] K. Matsuda, I. Hirabayashi, K. Kawamoto, T. Nabatame, T. Tokizaki, and A. Nakamura, *Phys. Rev. B* **50**, 4097 (1994).
- [39] H. Okamoto, T. Miyagoe, K. Kobayashi, H. Uemura, H. Nishioka, H. Matsuzaki, A. Sawa, and Y. Tokura, *Phys. Rev. B* **82**, 060513 (2010).
- [40] H. Okamoto, T. Miyagoe, K. Kobayashi, H. Uemura, H. Nishioka, H. Matsuzaki, A. Sawa, and Y. Tokura, *Phys. Rev. B* **83**, 125102 (2011).
- [41] F. Novelli, G. De Filippis, V. Cataudella, M. Esposito, I. Vergara, F. Cilento, E. Sindici, A. Amaricci, C. Giannetti, D. Prabhakaran, *et al.*, *Nature communications* **5**, 5112 (2014).
- [42] F. Cilento, G. Manzoni, A. Sterzi, S. Peli, A. Ronchi, A. Crepaldi, F. Boschini, C. Cacho, R. Chapman, E. Springate, H. Eisaki, M. Greven, M. Berciu, A. F. Kemper, A. Damascelli, M. Capone, C. Giannetti, and F. Parmigiani,

- Science Advances **4** (2018), 10.1126/sciadv.aar1998, <http://advances.sciencemag.org/content/4/2/eaar1998.full.pdf>.
- [43] B. Mansart, J. Lorenzana, A. Mann, A. Odeh, M. Scaronigella, M. Chergui, and F. Carbone, Proceedings of the National Academy of Sciences **110**, 4539 (2013).
- [44] C. Giannetti, F. Cilento, S. Dal Conte, G. Coslovich, G. Ferrini, H. Molegraaf, M. Raichle, R. Liang, H. Eisaki, M. Greven, *et al.*, Nature communications **2**, 353 (2011).
- [45] V. Emery, Physical Review Letters **58**, 2794 (1987).
- [46] S. Biermann, F. Aryasetiawan, and A. Georges, Phys. Rev. Lett. **90**, 086402 (2003).
- [47] T. Ayrál, S. Biermann, and P. Werner, Phys. Rev. B **87**, 125149 (2013).
- [48] L. Huang, T. Ayrál, S. Biermann, and P. Werner, Phys. Rev. B **90**, 195114 (2014).
- [49] P. Sun and G. Kotliar, Phys. Rev. B **66**, 085120 (2002).
- [50] R. Loudon, *The quantum theory of light* (OUP Oxford, 2000).
- [51] D. Golež, M. Eckstein, and P. Werner, (in preparation).
- [52] T. Ayrál, S. Biermann, P. Werner, and L. Boehnke, Phys. Rev. B **95**, 245130 (2017).
- [53] R. Sensarma, D. Pekker, E. Altman, E. Demler, N. Strohmaier, D. Greif, R. Jördens, L. Tarruell, H. Moritz, and T. Esslinger, Phys. Rev. B **82**, 224302 (2010).
- [54] Z. Lenarčič and P. Prelovšek, Phys. Rev. B **90**, 235136 (2014).
- [55] P. Werner, K. Held, and M. Eckstein, Phys. Rev. B **90**, 235102 (2014).
- [56] We have checked that for high-frequency excitations the shape of the spectra after the pulse is essentially the same.
- [57] C. Giannetti, M. Capone, D. Fausti, M. Fabrizio, F. Parmigiani, and D. Mihailovic, Adv. Phys. **65**, 58 (2016).
- [58] L. Boehnke, F. Nilsson, F. Aryasetiawan, and P. Werner, Phys. Rev. B **94**, 201106 (2016).
- [59] F. Nilsson, L. Boehnke, P. Werner, and F. Aryasetiawan, Phys. Rev. Materials **1**, 043803 (2017).